


RESEARCH

Open Access



The compositional and functional imbalance of the gut microbiota in CKD linked to disease patterns

Jing Li^{1,2†}, Yang Shen^{3†}, Kaixin Yan^{1,2}, Siyuan Wang^{1,2}, Jie Jiao^{1,2}, Hongjie Chi^{1,2}, Jiu-chang Zhong^{1,2}, Ying Dong^{1,2*}  and Pan Wang^{1,2*}

Abstract

Background The prevalence of chronic kidney disease (CKD) is on the rise, posing a significant public health challenge. Although gut microbiome dysbiosis has been implicated in the impairment of kidney functions, the existence of pathological subtypes-linked differences remains largely unknown. We aimed to characterize the intestinal microbiota in patients with membranous nephropathy (MN), IgA nephropathy (IgAN), minimal change disease (MCD), and ischemic renal injury (IRI) in order to investigate the intricate relationship between intestinal microbiota and CKD across different subtypes.

Methods We conducted a cross-sectional study involving 94 patients with various pathological patterns of CKD and 54 healthy controls (HCs). The clinical parameters were collected, and stool samples were obtained from each participant. Gut microbial features were analyzed using 16S rRNA sequencing and taxon annotation to compare the HC, CKD, MN, IgAN, MCD, and IRI groups.

Results The CKD subjects exhibited significantly reduced alpha diversity, modified community structures, and disrupted microbial composition and potential functions compared to the control group. The opportunistic pathogen *Klebsiella* exhibited a significant enrichment in patients with CKD, whereas *Akkermansia* showed higher abundance in HCs. The study further revealed the presence of heterogeneity in intestinal microbial signatures across diverse CKD pathological types, including MN, IgAN, MCD, and IRI. The depression of the family *Lachnospiraceae* and the genus *Bilophila* was prominently observed exclusively in patients with MN, while suppressed *Streptococcus* was detected only in individuals with MCD, and a remarkable expansion of the genus *Escherichia* was uniquely found in cases of IRI. The study also encompassed the development of classifiers employing gut microbial diagnostic markers to accurately discriminate between distinct subtypes of CKD.

Conclusions The dysregulation of gut microbiome was strongly correlated with CKD, exhibiting further specificity towards distinct pathological patterns. Our study emphasizes the significance of considering disease subtypes when assessing the impact of intestinal microbiota on the development, diagnosis, and treatment of CKD.

[†]Jing Li and Yang Shen contributed equally to this work.

*Correspondence:

Ying Dong
dongying91@foxmail.com
Pan Wang
diudiupan@163.com

Full list of author information is available at the end of the article



Keywords Chronic kidney disease, Gut microbiota, Membranous nephropathy, IgA nephropathy, Minimal change disease, Ischemia renal injury

Background

Chronic kidney disease (CKD) as a significant global public health concern, has emerged as one of the leading causes of mortality, and impacts more than 800 million populations, which account for approximately 10% of the people worldwide [1]. According to the Global Burden of Disease Study, CKD resulted in 1.2 million death and 35.8 million disability-adjusted life-years in 2017, with 1.4 million cardiovascular disease-related deaths attributable to impaired kidney function [2]. The large burden imposed by CKD has been exacerbated, particularly in recent years following COVID-19 pandemic [3, 4]. And investigators indicated that CKD might become the 13th leading cause of death by 2030 and the fifth most prevalent cause of death by 2040 globally [5, 6]. This underscores the urgent need for enhanced understanding and effective management of CKD to mitigate its devastating impact on global health.

The intestinal microbiome has emerged as an important environmental factor in host-related disease. Recently, the strong association between a disordered gut bacteria and CKD is increasingly recognized [7–9]. In membranous nephropathy (MN), it has been highlighted that both the diversity and richness of the intestinal microbiota were significantly reduced. Furthermore, evidence from animal experiments suggests that perturbations in the gut microbiome may play a crucial role in the onset of MN [10]. Decreased alpha-diversity and altered microbial composition were observed in patients suffered from IgA nephropathy (IgAN), with striking expansion of *Escherichia-Shigella*, *Pseudomonas*, *Erysipelatoclostridium*, *Ruminococcaceae_UBA1819*, and *Ruminococcaceae_CAG-352* [11]. In parallel, fundamental shifts in microbial signatures were identified in patients with an advanced state of CKD [8]. For example, *Blautia* spp., *Dorea* spp., and *Eggerthellaceae* were dramatically elevated in patients with end-stage renal disease, but *Prevotella* and *Roseburia* were found to be depleted. Impaired gut homeostasis was characterized to be associated with CKD severity during disease progression [7]. Especially, *Ruminococcus bromii* was elucidated as a key contributor to the complex integrated network among gut microbiome, fecal and serum metabolites, implying its pivotal role in CKD progression [7]. In addition, previous research has shown that CKD patients possess a distinct intestinal mycobiome community compared to healthy individuals [12]. Collectively, these insights suggest a relationship between the gut microbiota and the

kidney dysfunction, which has been referred as the gut-kidney axis.

However, the common and specific signatures of gut dysbiosis in distinct CKD pathological patterns, such as MN and IgAN etc., are rarely taken into account when analyzing gut microbiome profiles. Given that the pathophysiological processes of CKD subtypes were not exactly the same, studies exploring the potential association between intestinal microbiota dysbiosis and the development CKD require a comparative understanding regarding different disease phenotypes. Moreover, noninvasive and reliably diagnose techniques other than current renal biopsy method are necessary for identify disparate CKD types. Hence, one of the primary goals of the present work is to reproduce, validate and confirm previous reported findings of disordered gut bacteria in patients with CKD. And meanwhile, we also aim to characterize the intestinal microbiota in MN, IgAN, minimal change disease (MCD) and ischemia renal injury (IRI) patients, investigate the crosstalk between different members of the gut microbiota, and further improve the present CKD diagnose strategies.

Methods

Study population, subject details and sample collection

In the present study, we conducted a cross-sectional, observational study and recruited a total of 148 participants with 54 healthy controls (HCs) and 94 patients diagnosed with CKD from the Department of Nephrology, Beijing Chaoyang Hospital, Capital Medical University, Beijing, China. Subjects with kidney structural or functional abnormalities persisting for more than 3 months were considered as CKD according to the criteria of KDIGO clinical practice guidelines [13]. Furthermore, patients with CKD were further categorized into MN (n = 54), IgAN (n = 25), MCD (n = 10) and IRI (n = 5) according to the pathological type based on histological examination [14]. Exclusion criteria included pregnancy, suffering from cancer, autoimmune diseases, arrhythmia, atrial fibrillation, myocardial infarction, heart failure, renal failure, stroke, peripheral artery disease, inflammatory bowel disease, diabetes mellitus, and having received renal replacement therapy within the past 3 months. Participants were also excluded if they received antibiotics, prebiotics, probiotic treatment or gastrointestinal surgeries in the preceding month.

The acquirement of all clinical parameters followed standardized procedures. All clinical parameters of the

participants are presented in Table S1 in the supplemental material. Stool samples from each participant were freshly harvested into collection containers on ice packs. The samples were transported to the laboratory and stored at -80°C until fecal DNA extraction.

The study was approved (Permit No. 2023-ke-730) by the Medical Ethics Committee of Beijing Chaoyang Hospital (Capital Medical University, Beijing, China) and was conducted in accordance with the principles of the Helsinki Declaration. Written informed consent was obtained from all patients prior to enrollment.

Histology

Histological examination of renal tissues, including periodic acid-schiff staining (PAS), periodic acid-silver methenamine (PASM) & Masson trichrome staining, immunohistochemical study (IHC) and immunofluorescence staining (IF) were performed at Institute of Kidney Disease in Peking University. The renal tissues of patients were harvested by nephrologist through renipuncture, and were fixed in 4% paraformaldehyde, embedded in paraffin and sectioned. The sections were stained with periodic acid schiff reagent to determine the changes in the kidney tissue structures. PASM & Masson staining was performed to observe the basal membrane lesions and extracellular matrix, Bauman capsule wall, vascular elastic membranes of arteries, and deposition site of fugalobin, fibrinoid necrosis and thrombosis [15].

For IHC staining with positive cells of PLA2R, sections were processed through deparaffinized, rehydration, antigen promised, endogenous peroxidase activity blockade, and were then incubated with antibodies at 4°C overnight. After secondary antibodies incubation, the section samples were stained with avidin–biotin complex and counterstained with hematoxylin. The staining was examined, and images were captured under a microscope (Nikon).

For IF targeting Complement C3, k light chain, λ light chain, Immunoglobulin G (IgG), Immunoglobulin A (IgA), fixed renal tissues were dehydrated with 20–30% sucrose, embedded in OCT, frozen, and sectioned. The sections were permeabilized with Triton X-100 and stained with antibodies specific to C3, k, λ , IgG, IgA respectively overnight at 4°C . Samples were then incubated with FITC-coupled secondary antibodies. The staining was examined under a fluorescence microscope (Nikon).

16S rRNA sequencing and taxon annotation

Total DNA was extracted from stool samples, with DNA quality assessed by 1.2% agarose gel electrophoresis, and quantification was performed using Nanodrop spectrophotometer. Following a barcode sequence added, the

variable region of rRNA gene was amplified through polymerase chain reaction (PCR). PCR reaction was performed with reaction buffer, GC buffer, dNTP, forward and reverse primers, DNA template, ddH₂O and Q5 DNA polymerase. The V3–V4 hypervariable regions of the bacterial 16S rRNA gene were amplified with primers 5'-ACTCCTACGGGAGGCAGCA-3' (338F) and 5'-GGACTACHVGGGTWTCTAAT-3' (806R). The condition for amplified reaction was initial denaturation 98°C 2 min, denaturation 98°C 15 s, annealing 55°C 30 s, extension 72°C 30 s, final extension 72°C 5 min, 10°C hold, and 25–30 cycles. Quantification of the amplified products was conducted using the Quant-iT PicoGreen dsDNA Assay Kit on Microplate reader (BioTek, FLx800). We prepared the library with Illumina TruSeq Nano DNA LT Library Prep Kit, and purified it by 2% agarose gel electrophoresis. On Agilent Bioanalyzer, the library was evaluated with Agilent High Sensitivity DNA Kit, quantified on Promega QuantiFluor system with Quant-iT PicoGreen dsDNA Assay Kit, and subsequently quantified with Quant-iT PicoGreen dsDNA Assay Kit on Promega QuantiFluor system, denatured to a single strand, and subjected to paired-end sequencing on Illumina Novaseq-PE250.

With the raw high-throughput sequencing data acquired, the primers were removed, and we filtered the raw data by mass, denoised and spliced the sequence with DADA2 method in QIIME2 software (version 2019.4). Under Greengenes database (Release 13.8, <http://greengenes.secondgenome.com/> comments), taxonomic annotation was performed with classify-sklearn methods (<https://github.com/QIIME2/q2-feature-classifier>). The ggtree package (R software) was utilized to generate the taxonomic tree based on the microbiome composition, encompassing kingdoms, phyla, classes, orders, families, genera and species. Only taxa nodes with a relative abundance exceeding the 0.5% threshold at their respective classification level are presented in the taxonomic tree.

Microbial diversity

For bioinformatics analysis, bacterial alpha-diversity parameters including Chao1 index, Simpson, Shannon index, Pielou index and Goods coverage was calculated with the QIIME2 software (version 2019.4) to examine the diversity and richness of the gut microbial community. Richness was indicated by Chao1 and observed species index, diversity was represented using Shannon and Simpson index, evenness was determined by Pielou's evenness index, and Good's coverage index was used to depict coverage. Kruskal–Wallis rank sum test was applied to perform comparison of alpha diversity indexes between groups. Rarefaction curves were obtained by randomly extracting a certain number of sequences from

each sample, and calculating the total number of operational taxonomic units (OTUs) that the sample contain and the relative abundance of each OTU in a given series of sequencing depths with the QIIME2 software. Curves tending to be flat indicate that the sequencing data amount is progressive and reasonable, with more data facilitating to generate few novel OTUs.

Beta diversity is a comparative analysis of the microbial community composition with between-habitat diversity. According to the OTU abundance of all the samples, Bray–Curtis distance was calculated with QIIME2 software to evaluate the beta diversity. The Adonis (PERMANOVA, permutational multivariate analysis of variance) was performed using QIIME2 to assess the statistical significance of difference between groups. Principal-coordinate analysis (PCoA) distance matrix was analyzed by permutational multivariate analysis, and the scatter plots based on beta diversity distance were performed using the *vegan* and *ggplot2* packages in R.

Functional annotation

Prediction for the gut microbial community's functional capabilities was performed with the phylogenetic investigation of communities by reconstruction of unobserved states (PICRUSt2) to generate the Kyoto Encyclopedia of Genes and Genomes (KEGG, <https://www.kegg.jp/>) ontology (KO) and enzyme (EC) profiles. Briefly, by blasting the 16S rRNA gene information in the OTUs to the microbial reference genome Greengene database, phylogenetic tree was constructed, and the gene function of their shared ancestor was inferred. Based on the copy number of the gene family corresponding to the reference sequence in the phylogenetic tree, the species with the closest sequence with the feature sequence was deduced and thus the copy number of its gene family was obtained. The gene family copy number was calculated according to the abundance of each sample characteristic sequence. The gene families were mapped to KEGG database, and the pathway information with the abundance data of metabolic pathways in each sample were obtained. Thus, the composition of the bacterial

community was mapped to the database, and the gene function prediction of the gut bacteria was performed.

Statistics analysis

Kmeans cluster analysis, STAMP plot (R, version 4.1.3; *doBy* package, 4.6.13; *ggplot2* package, 3.3.6), Mfuzz analysis (R, version 4.1.3; Mfuzz package, 2.54.0) and random Forest (R, version 4.1.3; *ggplot2* package, 3.3.3; *random forest* package, 4.7–1.1) were conducted using the OmicStudio tools at <https://www.omicstudio.cn/tool> [16]. The relative abundance of all taxa was compared between groups with linear discriminant analysis (LDA) effect size analysis (LEfSe) at the Galaxy online analysis platform (<http://huttenhower.sph.harvard.edu/galaxy/>), and P values were obtained from Kruskal–Wallis or Wilcoxon test. The *corrplot* package in R software was utilized to conduct Spearman's rank correlation analysis. Partial least squares structural equation modeling (PLS-SEM) was performed using the Smart-PLS 3 software (version 4.0.0).

Results

Demographics and basic characteristics of all participants in the study cohort

The basic characteristics of the study cohort were summarized in Table S1. The CKD patients exhibited extremely higher systolic blood pressure, diastolic blood pressure, heart rate, total cholesterol, triglyceride and low-density lipoprotein cholesterol compared to HCs. Additionally, CKD patients displayed impaired kidney functions, as indicated by increased levels of serum creatinine, uric acid, and PH in urine. Conversely, the levels of creatinine clearance rate and hemoglobin were significantly lower in CKD group. Particularly, there were no dramatic differences in age or sex between groups.

Gut microbiome profiles were altered in CKD patients

The most predominant bacteria identified in the study cohort belonged to the phyla Firmicutes, Actinobacteria, Bacteroidetes and Proteobacteria (Fig. 1A, B). Notably, our results showed that the microbial composition at phylum level was discrepant in CKDs compared to

(See figure on next page.)

Fig. 1 Phylum and genus level distribution of bacteria in the fecal microbiota of the present cohort consisting CKD cases and healthy control subjects (HC). **A, B** Bar graph depicting the structural distributions of fecal microbial communities at the phylum level in each sample (**A**) and each group (**B**). The relative abundances of all detected phyla were shown. **C** Circos plots described the constitution of top15 phyla in CKD and HC groups, which simultaneously demonstrated the distribution of each phylum in distinct groups. **D, E** Taxonomic classification at the genus level for each individual in the study cohort (**D**), and the CKD and healthy groups (**E**). Relative abundances of the top 20 most abundant gut genera are presented and the aggregate relative abundance of the remaining taxa was not shown. **F** Circular visualization for the relative proportion of the top 16 genera in CKD and HC groups. The distribution of each genus in distinct groups was also displayed. **G** Taxonomic tree showed the cladogram taxonomy of taxa, with relative abundance > 0.005 as the thresholds in each level from kingdom, phylum, class, order, family, genus and species. The pie chart for each branch node of the rank tree showed the composition proportion of the taxon unit in each group

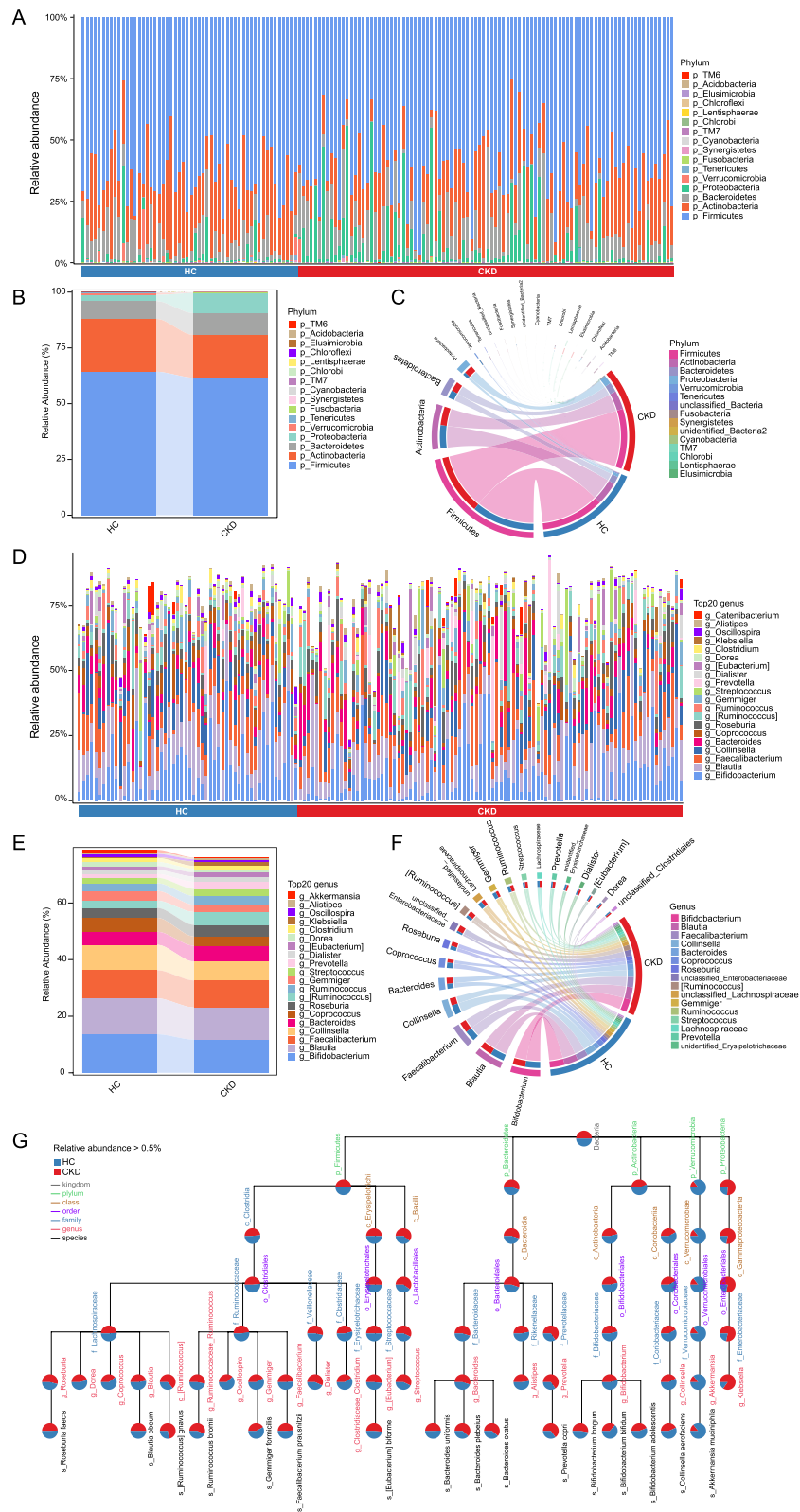


Fig. 1 (See legend on previous page.)

HCs, with CKD patients characterized by enhanced Proteobacteria and Bacteroidetes, along with a decrease in Actinobacteria and Firmicutes (Fig. 1B–C). The average compositions and relative abundances of the bacterial communities in CKDs and HCs at genus level were further described in Fig. 1D–F. And we observed considerable differences in the gut microbial profiles between the CKD and HC groups from the genus levels, with the abundance of *Bacteroides*, *Prevotella* and *Klebsiella* was enhanced in the CKD group, whereas *Bifidobacterium*, *Collinsella*, *Dorea*, *Oscillospira* and *Akkermansia* more abundant in the HC group (Fig. 1D–F). The detailed microbiome composition across various taxonomic levels as presented in the taxonomic tree from kingdoms, phyla, classes, orders, families, genera and species showed that, within the genera detected above, higher proportions of *Bacteroides plebeius*, *Bacteroides ovatus* and *Prevotella copri*, and lower proportions of *Bifidobacterium bifidum*, *Bifidobacterium adolescentis*, *Collinsella aerofaciens* and *Akkermansia muciniphila* in CKD patients (Fig. 1G).

We assessed the alterations in diversity of the intestinal microbiota in patients with CKD. Rarefaction curves based on observed OTUs in the groups nearly approached saturation as the sequencing depth increased, which meant a vast majority of taxa had been captured (Fig. 2B). Compared with HCs, the alpha-diversity of gut bacteria was statistically lower in patients with CKD, as evaluated by the observed species, Chao1 and Shannon index, which was consistent with the variations reported in previous studies of microbial populations in patients with CKD [10, 11, 17] (Fig. 2A). Additionally, the Simpson and Pielou indices were remarkably decreased whereas Goods coverage increase in CKD subjects. PCoA based on bray–curtis dissimilarity revealed a significant distinction in microbial community of CKD patients and HCs (Fig. 2C, $p=0.003$). The distribution of samples from CKD and HC based on the relative abundance of three most dominant phyla (Firmicutes, Actinobacteria and Bacteroidetes) also suggested disparity between groups (Fig. 2D). K-means clustering of genus-level features allowed the categorization of individuals into discrete clusters, represented by *Prevotella*, *Bifidobacterium* and *Faecalibacterium*, respectively (Fig. 2E). The distinct enrichment of groups in these clusters supported dysbiosis of intestinal environment in CKD patients.

The enriched genera of *Turicibacter* (from the family Turicibacteraceae and the order Turicibacterales), *Streptococcus* (from the family Streptococcaceae), *Enterobacter* and *Klebsiella*, as well as deficient *Butyricicoccus*, *Butyricimonas*, *Oscillospira*, *Gemmiger*, *Adlercreutzia*, *Coprococcus* and *Akkermansia* with high LDA scores emerged as key bacterial types contributing to gut microbiota dysbiosis in the CKD patients (Fig. 3A).

Concurrently, we performed STAMP analysis and confirmed the significant gut microbial changes at the genus level (Fig. 3B). The markedly lowered *Coprococcus*, *Adlercreutzia*, *Gemmiger*, *Oscillospira*, *Butyricimonas*, *Akkermansia*, *Butyricicoccus* and dramatically elevated opportunistic pathogens bacteria from *Turicibacter*, *Enterobacter*, *Klebsiella* and *Streptococcus* were elucidated (Fig. 3B). The co-occurrence correlation among the different gut microbial markers in the stamp analysis was further revealed by Spearman's rank correlation analysis (Fig. 3C). Meanwhile, a strong correlation between clinical parameters in laboratory examination and CKD-associated genera features was demonstrated (Figure S1). The key microbes differentially abundant between CKDs and HCs were linked to impaired renal functions and CKD severity (Figure S1A). Specially, the abundance of *Streptococcus* was positively correlated with blood urea nitrogen ($p=0.042$) and proteinuria ($p=0.032$). *Enterobacter* ($p=0.032$) and *Ruminococcus* ($p=0.01$) showed positive relationship with urine protein. Similarly, there was a positive correlation between *Mogibacterium* and creatinine ($p=0.047$).

Microbial function alterations in patients with CKD

We next evaluated the functional alterations of intestinal microbiome in CKD patients with those of HC. The composition profiles of KEGG enzymes, orthology and pathways were predicted on the basis of 16S rRNA sequencing data with PICRUSt2. Distinct patterns in the metabolic EC as well as KO of the gut microbiome were found in the CKDs as indicated by PCoA, and differential enrichment of multiple ECs and KOs between the two groups was identified based on LEfSe analysis (Figure S2A–D). In particular, the CKD group was characterized by the remarkable increase of nitrate reductase and 6-phospho-beta-glucosidase. Conversely, histidine kinase, [formate-C-acetyltransferase]-activating enzyme, glutamine synthetase, 3-oxoacyl-[acyl-carrier-protein] reductase and O-acetylhomoserine aminocarboxypropyltransferase etc. were depleted in patients with CKD compared with HCs.

At the pathway level, it was observed that the majority significantly varied metabolic KEGG pathways in CKDs was involved in metabolism, including lipid metabolism, amino acid metabolism, metabolism of cofactors and vitamins, carbohydrate and nucleotide (Figure S2E). Of note, the metabolic pathways participated in caprolactam degradation, biosynthesis of lipopolysaccharide, tropane, piperidine and pyridine alkaloid showed higher enrichment in CKDs (Figure S2E). In contrast, the essential microbial potentials involving in steroid, lysine, valine, leucine and isoleucine biosynthesis, histidine metabolism,

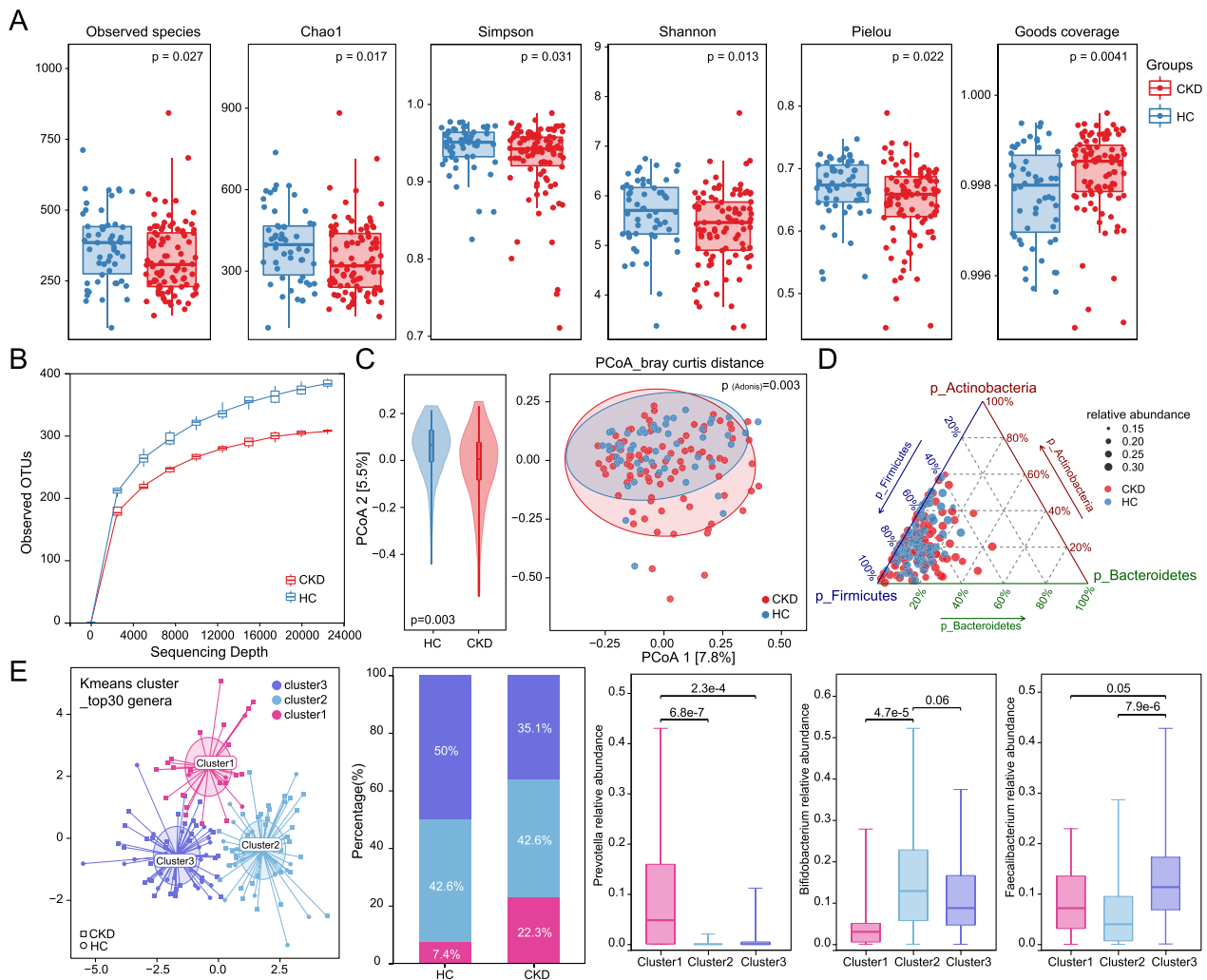


Fig. 2 Gut microbiome in CKD patients is characterized by depressed alpha diversity and heterogeneity in microbial beta diversity. **A** We showed differences in diversity and richness of the gut microbial community between CKD patients and healthy subjects. Number of observed species, and distribution of microbial alpha diversity such as Chao1 index, Simpson, Shannon, Pielou and Goods coverage index comparing CKD cases and healthy controls are shown. P values were computed by Wilcoxon rank test. Box-and-whiskers plots represent the interquartile ranges (25th through 75th percentiles, boxes), medians (50th percentiles, bars within the boxes), and the 5th and 95th percentiles (whiskers below and above the boxes). **B** Rarefaction curve in each group by gradually enhancing the sequencing depth of random samples and calculating the number of OTUs. The observed OTUs that the sample contains in a given series of sequencing depths were shown. **C** PCoA distance matrix based on bray curtis distance illustrated the heterogeneity of CKD patients and healthy subjects in between-habitat diversity. Different colors in the scatter plots represent samples from different groups. The higher the similarity between samples, the closer they distribute in the plots. Values in brackets represent the amount of total variability explained by each principal coordinates. P values were from the Adonis to test the significance of difference between groups. Violin plot depicted the distribution of single coordinate axis in PCoA2, with the difference obtained by wilcoxon rank sum test. **D** The distribution of CKD subjects and the controls was plotted in a ternary diagram based on the relative abundance of the top3 most dominant phylum (Actinobacteria, Firmicutes, and Bacteroidetes). **E** All the individuals were assigned into discrete clusters as identified by K-means clustering of genus-level features. The percentage of control and CKD samples distributed in cluster1, cluster2 and cluster3. There were 7.4% controls in cluster1, 50% controls in cluster3; 22.3% CKD participants in cluster1, 35.1% CKD patients in cluster3. Relative abundances of the top genera in each cluster were demonstrated, with *Prevotella* prominent in cluster1, *Bifidobacterium* dominant in cluster2 and *Faecalibacterium* in cluster3. Boxes represent the interquartile ranges, lines inside the boxes denote medians, and circles are outliers. P values were from the Kruskal–Wallis rank sum test

phenylalanine, tyrosine and tryptophan biosynthesis were overexpressed in HCs. The most significantly altered metabolic KEGG pathways in CKDs were

Valine, leucine and isoleucine biosynthesis (ko00290), Phenylalanine metabolism (ko00360), Biosynthesis of siderophore group nonribosomal peptides (ko01053),

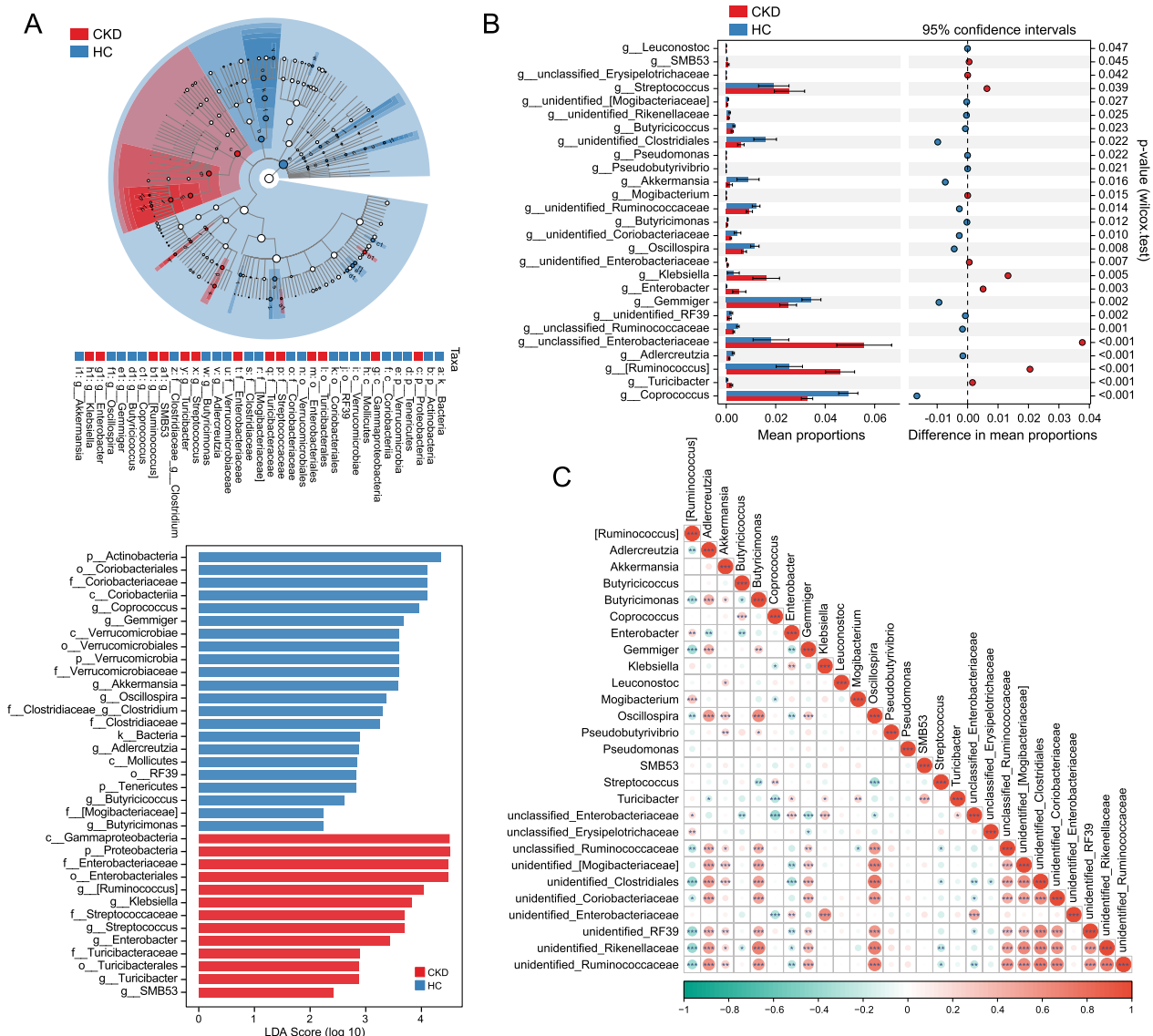


Fig. 3 Alterations of the microbial compositions in the cohort. **A** Linear discriminant analysis (LDA) effect size (LEfSe) analysis defined characteristically microbial taxa of CKD and HC groups based on LDA score > 2 and P value < 0.05. Cladogram showed the taxonomic tree and enriched groups of distinct taxa, with differential abundant taxonomic clades at phylum, class, order, family and genus level shown by successive circles from the inner to outer rings. **B** STAMP analysis showed comparison of significance of dominant bacteria at genus level of gut microbiota in the CKD and HC groups. **C** Heatmap elucidating the co-occurrence correlation between differently enriched taxonomic composition at the genus level in groups. Negative correlation is shown in green and positive correlation in red. *, P < 0.05; **, P < 0.01; ***, P < 0.001, Spearman's correlation

Nitrogen metabolism (ko00910) and Lysine biosynthesis (ko00300), respectively (Figure S3). These representative reaction pathways were further shown by referring to the KEGG pathway reference maps, and multiple KOs associated with CKD were marked based on fold changes (CKD/HC).

The gut microbiome community across different CKD disease phenotypes

To delve deeper into the patterns of gut microbiota dysbiosis specific to CKD disease phenotypes, the patients were classified into MN, IgAN, MCD and IRI, respectively, based on observations from pathological

examination (Fig. 4A). The patient demographics and renal function-related characteristics were described in Table S2, with approximate half of the patients diagnosed with MN, 26.60% with IgAN, 10.64% with MCD, and merely 5.32% with IRI.

To describe the heterogenous pathological features of CKD patients, renal biopsy was examined by PAS and PASM + Masson stainings. The results showed mesangial cells and stroma hyperplasia, diffuse basement membrane thickening and subepithelial fugalobin deposition in MN subjects. Their renal tubule epithelial cells were vacuolated and granular degeneration, and small focal atrophied (Fig. 4B). Fibrosis was detected in renal interstitial infiltration of small focal lymphocytes and monocytes, and the arteriole wall was thickened. Especially, PLA2R, C3, κ , λ , IgG, IgG1, IgG2 and IgG4 were also accumulated (Fig. 4B, Figure S4). For IgAN, the renal tubule epithelial cells were vacuolated and granular, with focal atrophy, and a few protein tubules were detected in the lumen, renal interstitial focal lymphoid and monocyte infiltration were observed with fibrosis, arteriole wall was thickening, and lumen was stenosis (Fig. 4B). The glomerular basement membrane of MCD was vacuolar degeneration, with renal tubular epithelial cells vacuole and granular degeneration (Fig. 4B). Renal tubular epithelial cell vacuolation and granular degeneration were observed in IRI patients, coupled with small focal atrophy, small focal lymphoid and monocyte infiltration in renal interstitium (Fig. 4B).

The microbiome characteristics of CKD pathological subtypes revealed that the pattern of microbial community composition was discriminative across groups both at phylum and genus level (Fig. 4C). Distribution of the top5 most dominant genera in disease phenotypes indicated particular dissimilarity with others in MCD and IRI (Fig. 4D). However, when compared with HCs, the alpha diversity (except for goods coverage) was significantly lower in MN, while it was slightly decreased in IgAN patients (marginal statistical difference), but the alpha diversity of MCD or IRI was similar to that of the controls

(Fig. 4E). In addition, microbiome community alterations in distinct CKD types were described by beta diversity with PCoA plot based upon bray–curtis dissimilarities (Fig. 4F), suggesting that pathological subtypes might be associated with specific microbial diversity. Comparisons were also performed between each pathological subtype and HC group, separately. Here, MN, MCD and IRI patients exhibited significantly discrimination from HCs, whereas not for IgAN (Fig. 4G–J).

Given these observations, we further characterized the microbial composition at genus level using Mfuzz analysis (Figure S5). Accordingly, we identified five cluster types significantly associated with the CKD disease pathological subtypes (Figure S5A). The identified microbial genera in the present cohort were assigned to different clusters according to relative abundance across groups, with 48 genera in Cluster1, 81 in Cluster2, 52 in Cluster3, 40 in Cluster4 and 66 in Cluster5, respectively. We found that, Cluster1 was mainly associated with samples from HC and was dominated by the commensal microbes such as *Coprococcus*, *Dorea*, *Butyricoccus* and *Coprobacillus* etc. (Figure S5B). Conversely, Cluster2~5 were mainly associated with samples from different pathological subtypes, and dominated by potential opportunistic pathogens, namely, *Prevotella*, *Klebsiella* and *Streptococcus*.

Significantly altered gut microbial profiles in disease phenotypes

Based on the microbial changes in CKD patients, we also examined differently abundant microbiota as potential markers of disease phenotype by LEfSe analysis (Fig. 5). The phylogenetic profiles of the bacterial taxa revealed that the taxonomic enrichment of *Klebsiella*, *Oxalobacter*, *Ruminococcus*, *Mogibacterium*, *Turicibacter* and *Enterobacter*, and lack of *Blautia*, *Butyricimonas*, *Odoribacter*, *Akkermansia*, *Oscillospira* and *Butyricoccus* contributed the most to the difference in gut microbiota between patients with MNs and HCs (Fig. 5A). Notably, the abundance of *Ruminococcus* and *Clostridium* was significantly higher in

(See figure on next page.)

Fig. 4 Alterations of gut microbial constructions among CKD cases with distinct pathological types. **A** The CKD patients in the present cohort were classified into MN (n = 54, 57.44%), IgAN (n = 25, 26.60%), MCD (n = 10, 10.64%) and IRI (n = 5, 5.32%) on the basis of pathological observations. **B** Representative images of renal tissues from CKD patients with MN, IgAN, MCD and IRI were obtained by PAS and PASM + Masson staining, respectively. IHC targeting M-type phospholipase A2 receptor (PLA2R) was performed in MN patients. Scale bars were 50 μ m. **C** Bar plots displaying the relative abundance of the microbiota phyla and top 20 most abundant genera in distinct phenotypic groups. **D** The distribution according to relative abundance of top 5 genera detected in distinct phenotypic groups was exhibited in radar charts. The relative abundance was scaled from 0 to 0.16. **E** Microbial alpha diversity in pathological types was measured on number of taxa, Chao1 index, Simpson, Shannon, Pielou index and Goods coverage, respectively. **F** PCoA plots based on the bray–curtis similarity among the gut microbiome from different pathological types in CKD patients. P values were from the Adonis to test the significance of difference among groups. Kruskal–Wallis rank sum test was used to determine the significance of distributions in PCoA2. **G–J** The PCoA analysis based on bray curtis distance was performed between each CKD pathological type and HC

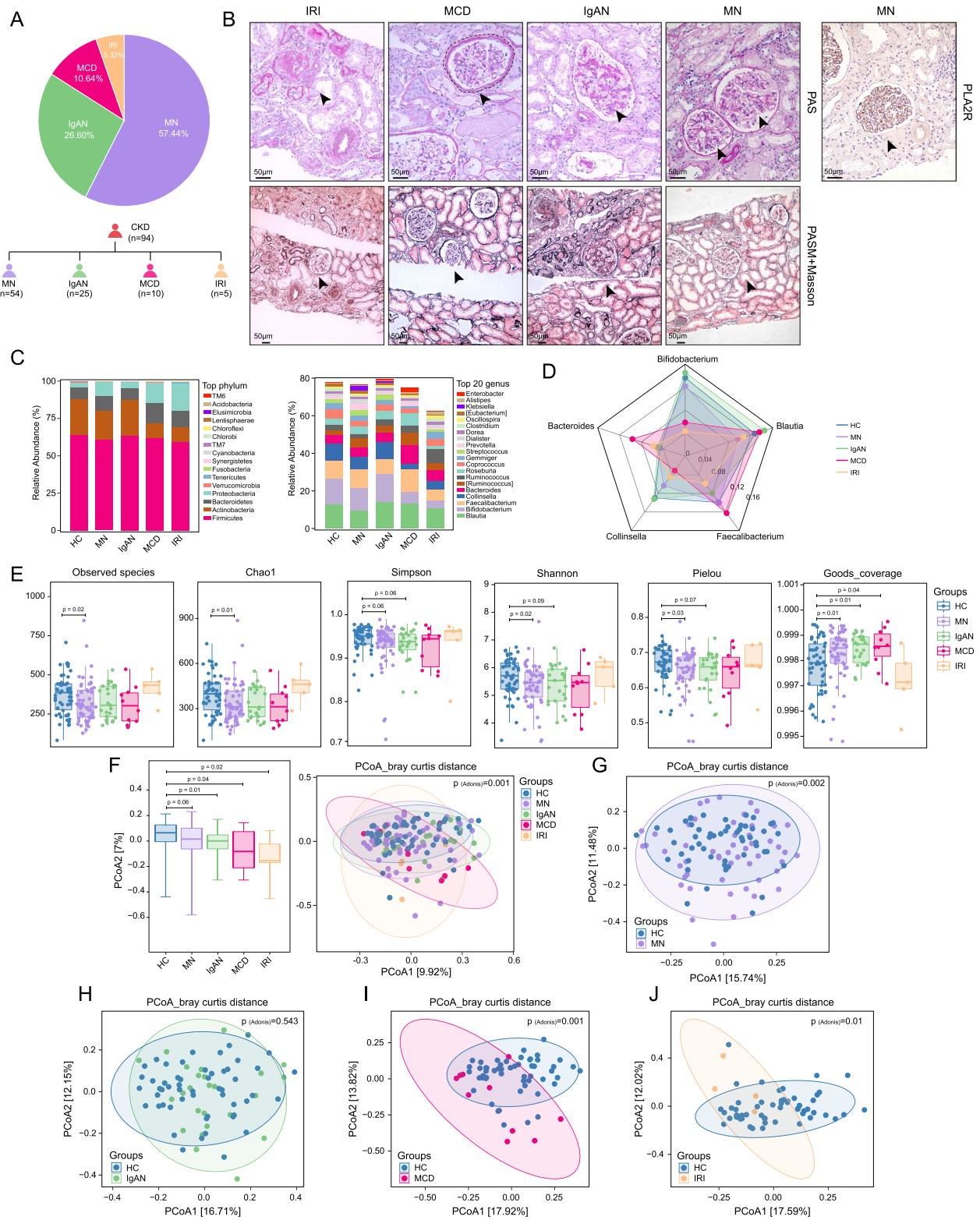


Fig. 4 (See legend on previous page.)

IgAN group, and *Akkermansia* was markedly depleted (Fig. 5B). Genera including *Rhizobium*, *Rudanella*, *Ruminococcus* and *Ralstonia* were identified at higher relative abundance in the MCD subjects, and *Bifidobacterium*, *Coprococcus*, *Gemmiger* and *Adlercreutzia* exhibited lower abundance levels (Fig. 5C). Meanwhile, *Acidaminococcus* decreased in the IRI group, while *Desulfovibrio*, *Klebsiella*, *Escherichia*, *Enterococcus*, *Anaerofilum* increased (Fig. 5D).

Among the enriched bacteria in each group, 12 MN-specific species were identified, including *Oxalobacter*, *Mogibacterium*, *Turicibacter* and *Enterobacter* (Fig. 6A). *Clostridium* was identified as a differential marker only enriched in IgAN. *Ralstonia*, *Rudanella* and *Rhizobium* were specifically abundant in MCD, whereas *Parabacteroides*, *Enterococcus*, *Escherichia*, *Desulfovibrio* etc. were particularly prevalent in the IRI group.

On the other side, 33 taxa such as *Butyricoccus*, *Parabacteroides*, *Alistipes*, *Oscillospira*, *Odoribacter* and *Butyricimonas* were uniquely depleted in MN patients, and *Actinomyces* was in IgAN (Fig. 6B). Nine microorganisms including *Streptococcus*, *Collinsella* and *Bifidobacterium* and 4 including *Acidaminococcus* were deficient specifically in MCD and IRI, respectively. The abundance of most significantly altered microbes associated with MN, IgAN, MCD and IRI were further shown in Fig. 6C, D. These obvious changed bacteria taxa are likely to be related to the onset of distinct CKD pathological types.

Subsequently, we evaluated the mediation effect of gut microbes for the contribution to CKD disease, pathological status and renal functions (Figure S6). In the relationship between baseline clinical parameters and CKD disease status, significant mediation effects for the top 50 most predominant genera were detected, with mediated proportions ranging from 27.9% for CKD to 30.2% for pathological subtypes, and 33.3% for kidney functions (Figure S6A). To further inquire into whether there were potential mediation effects of serum variations on the association between gut microbes and CKD, additional mediation analysis was performed (Figure S6B). Serum changes in laboratory examination such as ALT, AST, fasting blood glucose, high-density lipoprotein cholesterol, Low-density lipoprotein cholesterol, total cholesterol, triglyceride were found to significantly mediated

34.86%, 42.12% and 50.54% of the association, respectively (Figure S6B).

Establishment of the diagnostic model for distinct CKD pathological types

Predictive models according to clusters derived from Mfuzz analysis, significantly different taxa obtained by LEfSe analysis, and biomarkers identified with random forest (RF) were built, and receiver operating characteristic (ROC) curves for classifying each CKD pathological type from the others were developed (Figure S7). The results indicated that clusters derived from Mfuzz exhibited moderate distinguishing capabilities between MN and non-MN (AUC=74.3%), and IgAN and non-IgAN (AUC=71.1%), and enhanced accuracy for MCD (AUC=94.2%) and IRI (AUC=98.9%), respectively (Figure S7A). Compared with Mfuzz model, the LEfSe biomarkers had greater performances for MN (AUC=77.1%) and IgAN (AUC=78.7%) subjects, yet attenuated power for MCD and IRI (Figure S7B). Notably, the RF model based on bacterial features performed well with good accuracy (AUC=90.0% for MCD; AUC=91.7% for IRI), but relative lower diagnostic efficacy for MN (AUC=79.1%) and IgAN (AUC=60.9%) (Figure S7C, D), indicating that the model was not suitable for all CKD states. Together, these data suggested the RF bacterial classifier may have diagnostic potential as a noninvasive tool in distinguishing patients with CKD pathological types. However, the model had different performances in discriminating the risks of each subtype from the others.

Discussion

Recent insights have indicated that gut microbial dysbiosis is strongly associated with CKD disorders in patients [18], while the potential role of the intestinal tract and its microbiota in distinct pathological types is poorly understood. Here, we validated the significant alterations of the gut microbiome in our study cohort of CKD, characterized by decreased alpha diversity, altered microbial community structures, perturbed composition, and enhancement of multiple bacterial functions. Moreover, we revealed for the first time that the homogeneity and heterogeneity of intestinal microbial characteristics in different CKD pathological types, including MN, IgAN,

(See figure on next page.)

Fig. 5 Crucial taxa that contribute to the difference between patients with MN, IgAN, MCD and IRI and HCs on the basis of LDA effect size analysis. **A** Cladogram and bar chart shows crucial bacteria associated with MN. Taxa with an LDA value > 2 and P value < 0.05 in the MN and HC groups are marked with colors. **B** LEfSe identified the taxa with the greatest differences in abundance between the IgAN patients and the HCs. Taxa meeting a significant LDA threshold value of > 2 and P value < 0.05 were shown. **C** LEfSe analysis defined characteristically enriched microbial taxa in MCD and HC groups. **D** Significant different taxa between IRI and HC determined through the LEfSe analysis carried out with bacterial abundances

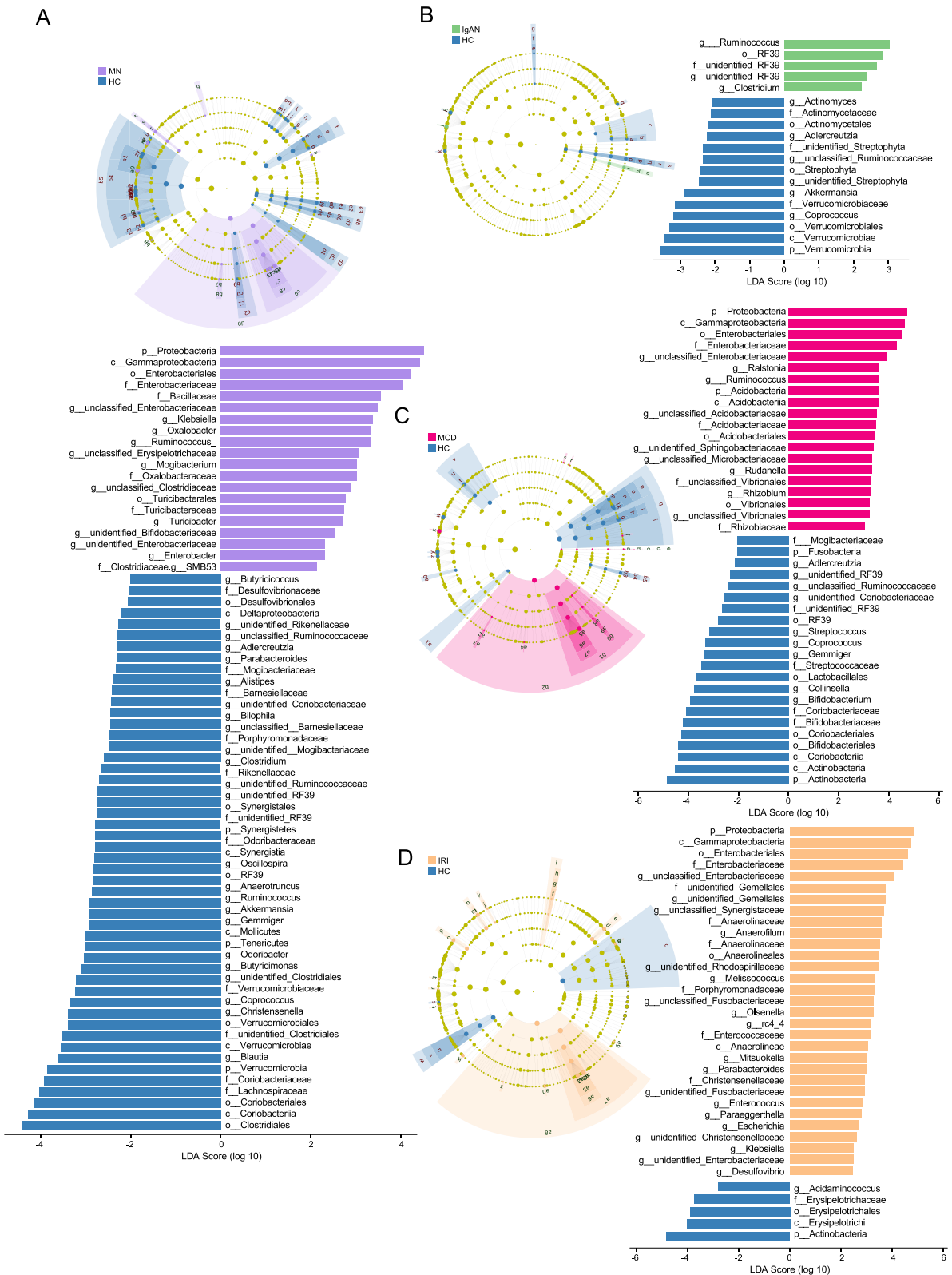


Fig. 5 (See legend on previous page.)

MCD and IRI. Notably, we constructed reliable classifiers to discriminate different CKD subtypes and determine the potential of gut microbial factors as noninvasive diagnostic markers.

Previously, available data have profiled the intestinal microbiota in patients with CKD, suggesting a decline in microbial diversity coupled with remarkably distinguished microbial community [19, 20]. These fundamental alterations within gut environment were detected in the present cohort consisting CKD patients and HCs, such as significantly depressed chao1, simpson, shannon and pielou indexes, and dramatically disparate features in beta-diversity. In parallel, we identified less CKD patients to be distributed in the cluster types dominant by the genus *Faecalibacterium*. Of note, butyrate-producing bacteria *Faecalibacterium* and *F. prausnitzii* have been suggested to be significantly depleted in CKD patients, and even more markedly reduced among end-stage kidney disease patients [21–24]. And higher eGFR was demonstrated to be positively associated with greater abundance of species from *Faecalibacterium* [23, 25]. Most recently, supplementation of *F. prausnitzii* was proved to exert beneficial effects in reducing renal dysfunction, renal inflammation, and lowering the serum levels of various uremic toxins, coupled with improving gut microbial ecology and intestinal integrity by production of butyrate through the G protein-coupled receptor-43 [26]. Collectively, these reports highlight the importance of gut dysbiosis, particularly *Faecalibacterium* in patients with CKD, which is also coincident with our findings. The consistency of our findings with previous reported observations by other investigators supported the imbalanced gut microbiome in patients suffering from CKD, and confirmed the reliability of our current study.

Meanwhile, our analyses that examined the prominently changes in CKD patients uncovered several core genera including an enrichment of opportunistic pathogen *Klebsiella* and a depletion of the important probiotic *Akkermansia*. Studies have reported that these bacteria are especially relevant for patients with CKD. For instance, an elevated colonization of *Klebsiella* was simultaneously detected in the human and canine gut

microbiome in CKD [20, 27]. And increase in the relative levels of genus *Klebsiella* was identified in the gut microbiota of patients with CKD at distinct stages [28], which further highlighted the importance of *Klebsiella* during CKD progression. In addition, the abundance of *Akkermansia* in the CKD group was suggested to be significantly lower than that in the HC group [29, 30]. Evidence based on experimental animals indicated *Akkermansia muciniphila* administration restored intestinal microecology, enhanced intestinal mucosal barrier function, and reduced renal interstitial fibrosis [31]. Whereas there are also some conflicting results that another report indicated that *Akkermansia* were increased with CKD progression [20]. These diverse clinical observations might reflect variations in patient characteristics, study sample sizes, baseline kidney function status etc.

Alterations in the microbiome, determined from analyses of fecal and intestinal samples, have been associated with CKD [32]. Unsurprisingly, endeavors aimed at modulating intestinal microbiota for therapeutic purposes have attracted wide attention from the scientific community. Li et al. demonstrated that supplementation of *F. prausnitzii* to CKD mice ameliorated renal dysfunction, attenuated renal inflammation, and decreased the serum levels of various uremic toxins [26]. Furthermore, Lee et al. reported that the depletion of intestinal microbiota depletion induced by antibiotics can attenuate the acute kidney injury to chronic kidney disease transition [33]. In the present study, we observed a significant association between dysregulation of the gut microbiome and CKD, exhibiting further specificity towards distinct pathological patterns. In the future, the specificity of intestinal microbiota may play a pivotal role in the diagnosis and treatment of CKD and its associated nephropathy subtypes.

The impacts of intestinal bacteria on the host frequently depend on the crosstalk with metabolism. In terms of the metabolic potentials of gut microbes in CKD, we observed enhanced capacity in lipopolysaccharide biosynthesis, glutathione metabolism and nitrogen metabolism etc. Among these functional pathways, lipopolysaccharide was the most well-known inducer for inflammation, fibrosis and injuries in renal epithelial

(See figure on next page.)

Fig. 6 Taxa specifically enriched or depleted in MN, IgAN, MCD and IRI as compared with HCs. **A** Venn diagram of differential microbial taxa (identified by LEfSe analysis) enhanced in MN patients vs. healthy controls, IgAN subjects vs. healthy controls, MCD subjects vs. healthy controls, and IRI subjects vs. healthy controls, respectively. Bar plot showed the total number of up-regulated taxa in each group. The taxa specifically enriched in MN, IgAN, MCD and IRI were listed, respectively. **B** Venn diagram showed microbial taxa significantly deficient in MN patients vs. healthy controls, IgAN subjects vs. healthy controls, MCD subjects vs. healthy controls, and IRI subjects vs. healthy controls. Bar plot showed the total number of down-regulated taxa in each group. The taxa specifically depleted in each group were listed, respectively. **C, D** Relative abundance of the top 4 most discriminative (according to P value) taxa specifically enhanced (**C**) or depressed (**D**) in MN, IgAN, MCD and IRI as compared with HCs

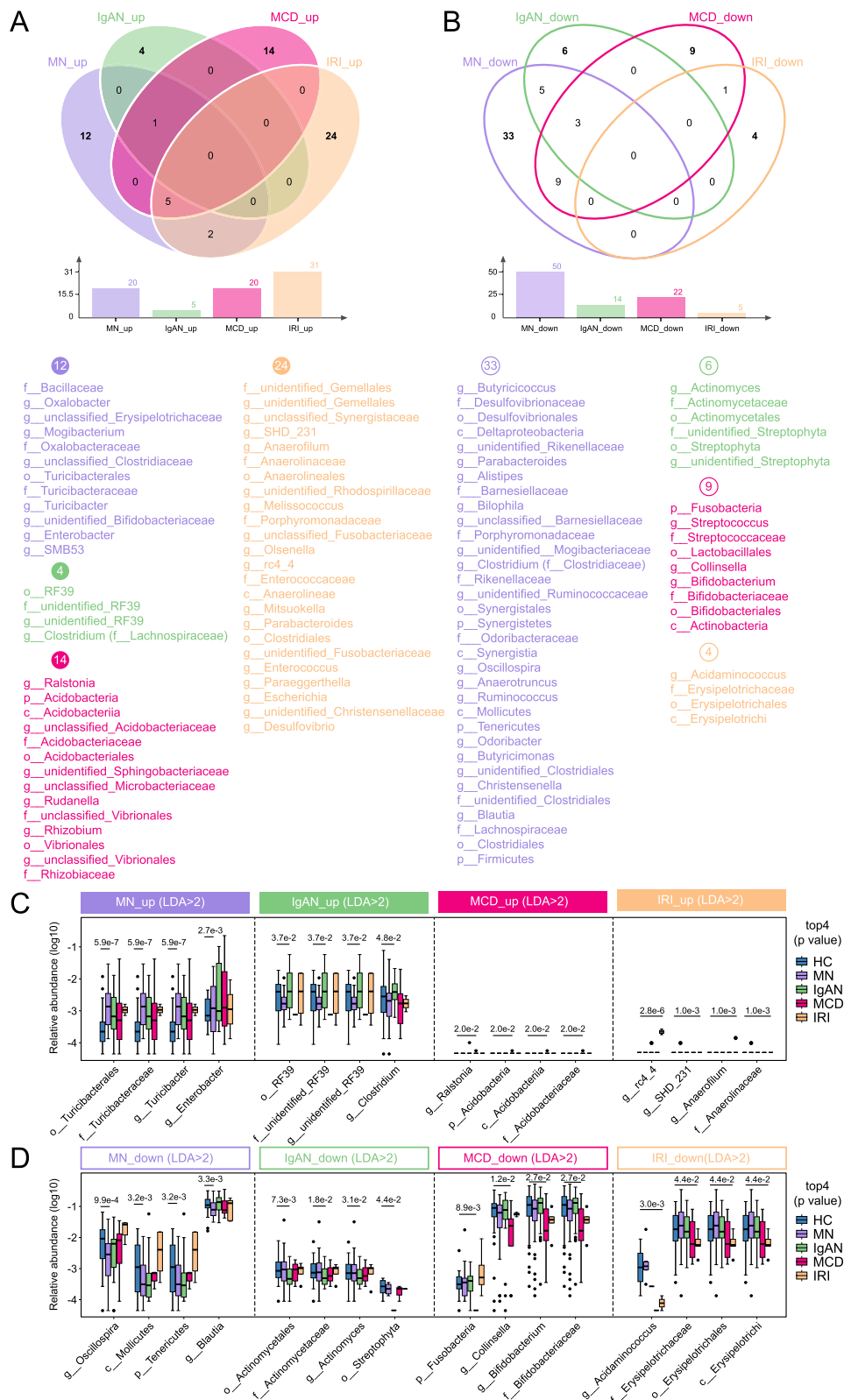


Fig. 6 (See legend on previous page.)

cells [34]. The production of lipopolysaccharides by gut microbiota has been demonstrated to be involved in the pathogenesis of CKD and even cardiovascular diseases [35]. The translocation of bacterial lipopolysaccharide from the intestinal lumen into the bloodstream was considered as a source of chronic inflammation in CKD [36]. In addition, the enrichment of bacterial gene markers related to glutathione metabolism was previously noted in CKD patients with a low protein diet [37]. Functional alteration in glutathione metabolism was identified to be accompanied with perturbed gut microbiome during CKD progression, showing close correlation with the specific microbial species that changed with CKD severity [7]. Notably, variations in glutathione metabolism pathway have been partially attributed to an increase in *Enterobacteriaceae* species that possess oxidizing substance-producing enzymes [7]. It was coincident that, our results also observed an overgrowth of family *Enterobacteriaceae* in CKD patients, indicating the contribution of gut microbes to metabolism. Furthermore, the end products of nitrogen metabolism, such as urea and creatinine, have been implicated in promoting kidney injuries [38]. The excessive potentials of intestinal microbiota in nitrogen metabolism detected in CKD patients, might participate in the secretion and accumulation of urea in body biological fluids [39], aggravating the burden on kidneys for urea elimination, and impairing renal functions.

In the present study, an in-depth understanding of microbial features in distinct pathological subtypes of CKD was further obtained, with various degrees of shifts in both alpha and beta microbial diversity of MN, IgAN, MCD and IRI identified, respectively. These findings underscore the remarkable heterogeneity in the gastrointestinal tract environment among distinct CKD subtypes, emphasizing the importance of underlying mechanisms, although the cause and consequence of gut dysbiosis remain unclear. Importantly, the etiology of CKD was widely known to be disparate in pathological types. MN was described with enhanced thickened glomerular basement membrane caused by the deposition of subepithelial immune complexes such as IgG and complement C3 [40], and positive detection of PLA2R. And IgAN patients were reported to exhibit deposited IgA as granular or clumpy form in the mesangial region [41]. Moreover, MCD was known to be related to diffuse fusion of foot process under electron microscope [42]. While IRI patients showed arteriolar wall thickening, hyalinosis, lumen stenosis with glomerular ischemic shrinkage and sclerosis and focal tubular atrophy and renal interstitial fibrosis [43–45].

Hence, the universal alterations and specific characteristics in microbial composition across pathological subtypes of CKD were determined. Our findings revealed

prominent biological heterogeneity in microbiome by pathology sub-typing. In MN patients, genus from *Lachnospiraceae* was demonstrated to be significantly reduced as compared with HCs [10]. Notably, this depletion of family *Lachnospiraceae* was unique to the MN group, and was absent in IgAN, MCD or IRI patients. The obvious changed bacteria taxa in *Lachnospiraceae* were likely to be related to the onset and pathology of MN. It was quite interesting that, the striking expansion of genus *Escherichia*, which has been regarded as a hallmark of IgAN, was previously shown to be the optimal bacterial classifier of IgAN, but not for distinguishing IgAN from MN [11]. Whereas, we observed the enrichment of *Escherichia* uniquely in IRI patients, and *Escherichia* was applied as one of the most important biomarkers in RF model classifier to identify IRIs from HCs. Moreover, a previous study investigating the gut bacterial communities included CKD patients with MN and IgAN [46]. The comparison performed between these groups indicated a higher abundance of *Bilophila*, whereas a depressed enrichment of *Streptococcus* in patients with IgAN than in those with MN [46]. In the current study, genus *Bilophila* was observed to be uniquely reduced in CKD patients diagnosed with MN, which support previous reports. However, the suppressed *Streptococcus* was detected merely in patients with MCD. Collectively, these findings indicate that future studies of gut microbiota composition and function in CKD will benefit from the inclusion of relevant subtypes to ensure the biological and clinical relevance of any uncovered host-microbiota correlations and associations within the clinical context.

However, there remain certain limitations inherent to this study. Firstly, as a single-center study with a relatively small sample size, it is imperative to conduct extensive studies involving larger sample sizes and multiple centers to replicate and further validate the alterations in profiles of microbiota among patients with CKD. Additionally, the drugs have been proposed to modulate the composition of the intestinal microbiome, and conversely, gut organisms can also influence the pharmacological properties of medical drugs [47]. The bidirectional interaction between oral antidiabetic drugs and the gut microbiota has been confirmed in patients with type 2 diabetes, exemplifying a significant relationship [48]. The anti-hypertensive drug, Amlodipine, has been shown to alleviate non-alcoholic fatty liver disease through the modulation of gut microbiota [49]. Although subjects with diabetes mellitus and those who have received antibiotics, prebiotics, or probiotics have been excluded, the use of antihypertensive medications or drugs targeting CKD may still introduce confounding factors in this study. Unanswered questions persist regarding the impact of drug usage on the observed bacterial characteristics in CKD patients,

underscoring the imperative for further research to substantiate and expand upon our findings through a clinical trial involving CKD cohorts devoid of drug intervention.

Conclusions

Here, novel insights into the compositional and functional nature of gut microbiome changes in CKD disorders, especially in distinct pathological subtypes were emphasized in the current study. The linkage between intestinal dysbiosis and CKD pathophysiology of MN, IgAN, MCD and IRI was covered. Bacterial taxa with specific distributions in the intestinal environment of CKD subtypes were identified, although much remains to be elucidated regarding their role and mechanisms in CKD pathogenesis. The potentials of gut microbiome in advancing the traditional clinical diagnosis strategies of CKD pathological subtypes were further demonstrated.

Abbreviations

CKD	Chronic kidney disease
HCS	Healthy controls
MN	Membranous nephropathy
IgAN	IgA nephropathy
MCD	Minimal change disease
IRI	Ischemia renal injury
PAS	Periodic acid-schiff staining
PASM	Periodic acid-silver methenamine
IHC	Immunohistochemical study
IF	Immunofluorescence staining
IgG	Immunoglobulin G
IgA	Immunoglobulin A
PCR	Polymerase chain reaction
PICRUSt2	Phylogenetic investigation of communities by reconstruction of unobserved states
KEGG	Kyoto Encyclopedia of Genes and Genomes
KO	KEGG ontology
EC	KEGG enzyme
LDA	Linear discriminant analysis
LEfSe	Linear discriminant analysis effect size analysis
RF	Random forest
ROC	Receiver operating characteristic

Supplementary Information

The online version contains supplementary material available at <https://doi.org/10.1186/s12967-024-05578-w>.

Supplementary Material 1.

Acknowledgements

None.

Author contributions

YD and PW conceived and designed the study. JL and YS contributed to literature search, conducted experiments and collected data. KY, SW, JJ, HC and JZ collected the clinical samples. JL and YS analyzed and interpreted the data. JL, YS, YD and PW wrote and revised the manuscript. YD and PW supervised all the processes in this manuscript. All the authors have read and agreed to the published version of the manuscript.

Funding

None.

Availability of data and materials

The datasets supporting the results of this study have been deposited in the National Center for Biotechnology Information under BioProject accession code PRJNA1088902 (<https://www.ncbi.nlm.nih.gov/sra/PRJNA1088902>).

Declarations

Ethics approval and consent to participate

The study was approved (Permit No. 2023-ke-730) by the Medical Ethics Committee of Beijing Chaoyang Hospital (Capital Medical University, Beijing, China) and was conducted in accordance with the principles of the Helsinki Declaration. Written informed consent was obtained from all patients prior to enrollment.

Consent for publication

Not applicable.

Competing interests

The authors declare no conflicts of interest related to this study.

Author details

¹Heart Center and Beijing Key Laboratory of Hypertension, Beijing Chaoyang Hospital, Capital Medical University, 8th Gongtinanlu Rd, Chaoyang District, Beijing 100020, China. ²Department of Cardiology, Beijing Chaoyang Hospital, Capital Medical University, Beijing, China. ³Department of Nephrology, Beijing Chaoyang Hospital, Capital Medical University, Beijing, China.

Received: 3 May 2024 Accepted: 4 August 2024

Published online: 16 August 2024

References

- Kovesdy CP. Epidemiology of chronic kidney disease: an update 2022. *Kidney Int Suppl* (2011). 2022;12(1):7–11.
- GBD Chronic Kidney Disease Collaboration. Global, regional, and national burden of chronic kidney disease, 1990–2017: a systematic analysis for the Global Burden of Disease Study 2017. *Lancet*. 2020;395(10225):709–33.
- Bouwman P, Malahe SRK, Messchendorp AL, Vart P, Imhof C, Sanders JF, Gansevoort RT, de Vries APJ, Abrahams AC, Bemelman FJ, Vervoort JPM, Hilbrands LB, Ten Dam MAGJ, van den Dorpel RMA, Rispens T, Steenhuis M, Reinders MEJ, Hemmelder MH, RECOVAC Consortium. Post COVID-19 condition imposes significant burden in patients with advanced chronic kidney disease: a nested case-control study. *Int J Infect Dis*. 2024;142:106990.
- Arborg A, Caldinelli A, Wijkström J, Nowak A, Fored M, Stendahl M, Evans M, Rydell H. Risk factors for COVID-19 hospitalization and mortality in patients with chronic kidney disease: a nationwide cohort study. *Clin Kidney J*. 2023;17(1):sfad283.
- Mathers CD, Loncar D. Projections of global mortality and burden of disease from 2002 to 2030. *PLoS Med*. 2006;3(11): e442.
- Foreman KJ, Marquez N, Dolgert A, Fukutaki K, Fullman N, McGaughey M, Pletcher MA, Smith AE, Tang K, Yuan CW, Brown JC, Friedman J, He J, Heuton KR, Holmberg M, Patel DJ, Reidy P, Carter A, Cercy K, Chapin A, Douwes-Schultz D, Frank T, Goettsch F, Liu PY, Nandakumar V, Reitsma MB, Reuter V, Sadat N, Sorensen RJD, Srinivasan V, Updike RL, York H, Lopez AD, Lozano R, Lim SS, Mokdad AH, Vollset SE, Murray CJL. Forecasting life expectancy, years of life lost, and all-cause and cause-specific mortality for 250 causes of death: reference and alternative scenarios for 2016–40 for 195 countries and territories. *Lancet*. 2018;392(10159):2052–90.
- Wang H, Ainiwaer A, Song Y, Qin L, Peng A, Bao H, Qin H. Perturbed gut microbiome and fecal and serum metabolomes are associated with chronic kidney disease severity. *Microbiome*. 2023;11(1):3.
- Zhang P, Wang X, Li S, Cao X, Zou J, Fang Y, Shi Y, Xiang F, Shen B, Li Y, Fang B, Zhang Y, Guo R, Lv Q, Zhang L, Lu Y, Wang Y, Yu J, Xie Y, Wang R, Chen X, Yu J, Zhang Z, He J, Zhan J, Lv W, Nie Y, Cai J, Xu X, Hu J, Zhang Q, Gao T, Jiang X, Tan X, Xue N, Wang Y, Ren Y, Wang L, Zhang H, Ning Y, Chen J, Zhang L, Jin S, Ren F, Ehrlich SD, Zhao L, Ding X. Metagenome-wide

- analysis uncovers gut microbial signatures and implicates taxon-specific functions in end-stage renal disease. *Genome Biol.* 2023;24(1):226.
9. Krukowski H, Valkenburg S, Madella AM, Garssen J, van Bergenhenegouwen J, Overbeek SA, Huys GRB, Raes J, Glorieux G. Gut microbiome studies in CKD: opportunities, pitfalls and therapeutic potential. *Nat Rev Nephrol.* 2023;19(2):87–101.
 10. Shang J, Zhang Y, Guo R, Liu W, Zhang J, Yan G, Wu F, Cui W, Wang P, Zheng X, Wang T, Dong Y, Zhao J, Wang L, Xiao J, Zhao Z. Gut microbiome analysis can be used as a noninvasive diagnostic tool and plays an essential role in the onset of membranous nephropathy. *Adv Sci (Weinh).* 2022;9(28): e2201581.
 11. Zhao J, Bai M, Ning X, Qin Y, Wang Y, Yu Z, Dong R, Zhang Y, Sun S. Expansion of *Escherichia-Shigella* in gut is associated with the onset and response to immunosuppressive therapy of IgA nephropathy. *J Am Soc Nephrol.* 2022;33(12):2276–92.
 12. Hu J, Wei S, Gu Y, Wang Y, Feng Y, Sheng J, Hu L, Gu C, Jiang P, Tian Y, Guo W, Lv L, Liu F, Zou Y, Yan F, Feng N. Gut mycobiome in patients with chronic kidney disease was altered and associated with immunological profiles. *Front Immunol.* 2022;13: 843695.
 13. Kidney Disease: Improving Global Outcomes (KDIGO) CKD Work Group. KDIGO 2024 clinical practice guideline for the evaluation and management of chronic kidney disease. *Kidney Int.* 2024;105(4):S117–314.
 14. Sethi S, Haas M, Markowitz GS, D'Agati VD, Rennek HG, Jennette JC, Bajema IM, Alpers CE, Chang A, Cornell LD, Cosio FG, Fogo AB, Glasscock RJ, Hariharan S, Kambham N, Lager DJ, Leung N, Mengel M, Nath KA, Roberts IS, Rovin BH, Seshan SV, Smith RJ, Walker PD, Winearls CG, Appel GB, Alexander MP, Cattran DC, Casado CA, Cook HT, De Vriese AS, Radhakrishnan J, Racusen LC, Ronco P, Fervenza FC. Mayo clinic/renal pathology society consensus report on pathologic classification, diagnosis, and reporting of GN. *J Am Soc Nephrol.* 2016;27(5):1278–87.
 15. Chang A, Gibson IW, Cohen AH, Weening JW, Jennette JC, Fogo AB, Renal Pathology Society. A position paper on standardizing the nonneoplastic kidney biopsy report. *Hum Pathol.* 2012;43(8):1192–6.
 16. Lyu F, Han F, Ge C, Mao W, Chen L, Hu H, Chen G, Lang Q, Fang C. OmicStudio: a composable bioinformatics cloud platform with real-time feedback that can generate high-quality graphs for publication. *Imeta.* 2023;2(1): e85.
 17. Li M, Wei L, Sun J, Zhu Q, Yang H, Zhang Y, Zhang C, Xi L, Zhao R, Du X. Association of gut microbiota with idiopathic membranous nephropathy. *BMC Nephrol.* 2022;23(1):164.
 18. Hu X, Ouyang S, Xie Y, Gong Z, Du J. Characterizing the gut microbiota in patients with chronic kidney disease. *Postgrad Med.* 2020;132(6):495–505.
 19. Chung S, Barnes JL, Astroth KS. Gastrointestinal microbiota in patients with chronic kidney disease: a systematic review. *Adv Nutr.* 2019;10(5):888–901.
 20. Ren Z, Fan Y, Li A, Shen Q, Wu J, Ren L, Lu H, Ding S, Ren H, Liu C, Liu W, Gao D, Wu Z, Guo S, Wu G, Liu Z, Yu Z, Li L. Alterations of the human gut microbiome in chronic kidney disease. *Adv Sci (Weinh).* 2020;7(20):2001936.
 21. Margiotta E, Miragoli F, Callegari ML, Vettoretti S, Caldiroli L, Meneghini M, Zanon F, Messa P. Gut microbiota composition and frailty in elderly patients with Chronic Kidney Disease. *PLoS ONE.* 2020;15(4): e0228530.
 22. Yang CY, Chen TW, Lu WL, Liang SS, Huang HD, Tseng CP, Tarng DC. Synbiotics alleviate the gut indole load and dysbiosis in chronic kidney disease. *Cells.* 2021;10(1):114.
 23. Jiang S, Xie S, Lv D, Zhang Y, Deng J, Zeng L, Chen Y. A reduction in the butyrate producing species *Roseburia* spp. and *Faecalibacterium prausnitzii* is associated with chronic kidney disease progression. *Antonie Van Leeuwenhoek.* 2016;109(10):1389–96.
 24. Li Y, Su X, Zhang L, Liu Y, Shi M, Lv C, Gao Y, Xu D, Wang Z. Dysbiosis of the gut microbiome is associated with CKD5 and correlated with clinical indices of the disease: a case-controlled study. *J Transl Med.* 2019;17(1):228.
 25. Peters BA, Qi Q, Usyk M, Daviglius ML, Cai J, Franceschini N, Lash JP, Gellman MD, Yu B, Boerwinkle E, Knight R, Burk RD, Kaplan RC. Association of the gut microbiome with kidney function and damage in the Hispanic Community Health Study/Study of Latinos (HCHS/SOL). *Gut Microbes.* 2023;15(1):2186685.
 26. Li HB, Xu ML, Xu XD, Tang YY, Jiang HL, Li L, Xia WJ, Cui N, Bai J, Dai ZM, Han B, Li Y, Peng B, Dong YY, Aryal S, Manandhar I, Eladawi MA, Shukla R, Kang YM, Joe B, Yang T. *Faecalibacterium prausnitzii* attenuates CKD via butyrate-renal GPR43 axis. *Circ Res.* 2022;131(9):e120–34.
 27. Kim KR, Kim SM, Kim JH. A pilot study of alterations of the gut microbiome in canine chronic kidney disease. *Front Vet Sci.* 2023;10:1241215.
 28. Chen TH, Liu CW, Ho YH, Huang CK, Hung CS, Smith BH, Lin JC. Gut microbiota composition and its metabolites in different stages of chronic kidney disease. *J Clin Med.* 2021;10(17):3881.
 29. Li F, Wang M, Wang J, Li R, Zhang Y. Alterations to the gut microbiota and their correlation with inflammatory factors in chronic kidney disease. *Front Cell Infect Microbiol.* 2019;9:206.
 30. Zhang J, Luo D, Lin Z, Zhou W, Rao J, Li Y, Wu J, Peng H, Lou T. Dysbiosis of gut microbiota in adult idiopathic membranous nephropathy with nephrotic syndrome. *Microb Pathog.* 2020;147: 104359.
 31. Pei T, Hu R, Wang F, Yang S, Feng H, Li Q, Zhang J, Yan S, Ju L, He Z, Han Z, Yang A, Xiao W, Ma Y, Wang M. Akkermansia muciniphila ameliorates chronic kidney disease interstitial fibrosis via the gut-renal axis. *Microb Pathog.* 2023;174: 105891.
 32. Knauf F, Brewer JR, Flavell RA. Immunity, microbiota and kidney disease. *Nat Rev Nephrol.* 2019;15(5):263–74.
 33. Lee J, Lee J, Kim K, Lee J, Jung Y, Hyeon JS, Seo A, Jin W, Weon B, Shin N, Kim S, Lim CS, Kim YS, Lee JP, Hwang GS, Yang SH. Antibiotic-induced intestinal microbiota depletion can attenuate the acute kidney injury to chronic kidney disease transition via NADPH oxidase 2 and trimethylamine-N-oxide inhibition. *Kidney Int.* 2024;105(6):1239–53.
 34. Zhou X, Yao Q, Sun X, Gong X, Yang Y, Chen C, Shan G. Slit2 ameliorates renal inflammation and fibrosis after hypoxia-and lipopolysaccharide-induced epithelial cells injury in vitro. *Exp Cell Res.* 2017;352(1):123–9.
 35. Suganya K, Son T, Kim KW, Koo BS. Impact of gut microbiota: How it could play roles beyond the digestive system on development of cardiovascular and renal diseases. *Microb Pathog.* 2021;152: 104583.
 36. Sun PP, Perianayagam MC, Jaber BL. Endotoxin-binding affinity of sevelamer: a potential novel anti-inflammatory mechanism. *Kidney Int Suppl.* 2009;114:S20–5.
 37. Wu IW, Lee CC, Hsu HJ, Sun CY, Chen YC, Yang KJ, Yang CW, Chung WH, Lai HC, Chang LC, Su SC. Compositional and functional adaptations of intestinal microbiota and related metabolites in CKD patients receiving dietary protein restriction. *Nutrients.* 2020;12(9):2799.
 38. Meola M, Nalesso F, Petrucci I, Samoni S, Ronco C. Pathophysiology and clinical work-up of acute kidney injury. *Contrib Nephrol.* 2016;188:1–10.
 39. Pundir CS, Jakhar S, Narwal V. Determination of urea with special emphasis on biosensors: a review. *Biosens Bioelectron.* 2019;123:36–50.
 40. Couser WG. Primary membranous nephropathy. *Clin J Am Soc Nephrol.* 2017;12(6):983–97.
 41. Cheung C, Bashir S, Barratt J. IgA nephropathy. *Br J Hosp Med (Lond).* 2014;75(Suppl 11):C173–6.
 42. Vivarelli M, Massella L, Ruggiero B, Emma F. Minimal change disease. *Clin J Am Soc Nephrol.* 2017;12(2):332–45.
 43. Adamczak M, Wiecek A. Ischemic nephropathy—pathogenesis and treatment. *Nefrologia.* 2012;32(4):432–8.
 44. Sharfuddin AA, Molitoris BA. Pathophysiology of ischemic acute kidney injury. *Nat Rev Nephrol.* 2011;7(4):189–200.
 45. Wenzel UO, Bode M, Köhl J, Ehmke H. A pathogenic role of complement in arterial hypertension and hypertensive end organ damage. *Am J Physiol Heart Circ Physiol.* 2017;312(3):H349–54.
 46. Dong R, Bai M, Zhao J, Wang D, Ning X, Sun S. A comparative study of the gut microbiota associated with immunoglobulin a nephropathy and membranous nephropathy. *Front Cell Infect Microbiol.* 2020;10: 557368.
 47. Verdegaaal AA, Goodman AL. Integrating the gut microbiome and pharmacology. *Sci Transl Med.* 2024;16(732):eadg8357.
 48. Ren H, Shi Z, Yang F, Wang S, Yuan F, Li T, Li M, Zhu J, Li J, Wu K, Zhang Y, Ning G, Kristiansen K, Wang W, Gu Y, Zhong H. Deciphering unique and shared interactions between the human gut microbiota and oral antidiabetic drugs. *Imeta.* 2024;3(2): e179.
 49. Li Y, Zhao D, Qian M, Liu J, Pan C, Zhang X, Duan X, Zhang Y, Jia W, Wang L. Amlodipine, an anti-hypertensive drug, alleviates non-alcoholic fatty liver disease by modulating gut microbiota. *Br J Pharmacol.* 2022;179(9):2054–77.

Publisher's Note

Springer Nature remains neutral with regard to jurisdictional claims in published maps and institutional affiliations.